

Short Communication

## Remediation of chromium contaminated soil by microbial electrochemical technology

Guan-Xi Li<sup>1,2</sup> He-Chuan Yang<sup>2</sup>, Shuai Guo<sup>1</sup>, Chao-Fan Qi<sup>1</sup>, Ke-Jing Wu<sup>1</sup> and Fen-Fen Guo<sup>1\*</sup>

<sup>1</sup> School of Life Sciences, Qufu Normal University, Shandong 273165, China

<sup>2</sup> Lianyungang Academy of Agricultural Sciences, Lianyungang, Jiangsu 222006, China

\*E-mail: [guoff@qfnu.edu.cn](mailto:guoff@qfnu.edu.cn)

Received: 17 February 2020 / Accepted: 5 April 2020 / Published: 10 June 2020

---

Soil is an irreplaceable resource for human survival and development. With the development of the heavy metal industry, heavy metal pollution of soil has become a serious problem that human beings are facing, especially soil pollution caused by hexavalent chromium. In this study, a plant microbial fuel cell (PMFC) system for the remediation of hexavalent chromium-contaminated soil was constructed by coupling plants and microbial fuel cells (MFCs). The removal efficiency of hexavalent chromium and the power generation capacity of the system were investigated. In this study, a new single-chamber PMFC was constructed, which was activated by *Lycoris radiata* and *Lycoris sprengeri*. Then, by controlling the HRT, open-circuit or closed-circuit conditions and the initial concentration of hexavalent chromium in the soil, the effects of these factors on the chromium removal efficiency of the PMFC system were analysed.

---

**Keywords:** Soil pollution; Phytoremediation; Plant microbial fuel cell; Hexavalent chromium; *Lycoris*

### 1. INTRODUCTION

With the development of science and technology, chromium and its compounds are widely used in production and life. The chromium industry has a wide range of sources, mainly in the printing and dyeing, leather tanning, metallurgy, electroplating and wood anticorrosion industries. Soil pollution caused by hexavalent chromium has become a serious environmental problem, especially in China. Chromium is one of the necessary trace elements for the human body and can exist in the natural environment in the form of trivalent and hexavalent elements. Compounds containing trivalent chromium and hexavalent chromium can transform each other under certain conditions. The toxicity of chromium is closely related to its valence state. Hexavalent chromium is an internationally recognized carcinogen [1–3]. Studies show that its biological toxicity is far greater than that of trivalent chromium. It is generally believed that the biological toxicity of hexavalent chromium compounds is 100 times higher than that of trivalent chromium compounds [4–6]. However, even among compounds containing

hexavalent chromium, the toxicity of different compounds is also very different. Trivalent chromium is an essential microelement for human beings. It participates in the normal metabolism of glucose and cholesterol and has the function of promoting insulin secretion [7,8]. In a certain concentration range, trivalent chromium can be considered to be non-toxic to the human body. Therefore, transforming hexavalent chromium with high toxicity into trivalent chromium with low toxicity is a good technique for reducing chromium pollution [9–12].

There are many insurmountable defects in traditional soil remediation technology, including excessive capital consumption and chemical residues, such as the soil replacement method, chemical adsorption and desorption method, and in situ leaching method [13–21]. In recent years, phytoremediation of heavy metal-contaminated soil has provided a new way to solve this problem. In the foreseeable future, phytoremediation has immeasurable potential in the treatment of heavy metal-contaminated soil, and there are abundant plant resources in nature; that is, many plants can be used in this technology [22–25].

At the same time, with the development of microbial fuel cell (MFC) technology, many kinds of MFC technology have been developed in recent years [26–35]. Plant MFCs (PMFCs) introduce plants into the MFC system and use plant rhizosphere secretion and other organic matter in soil to generate electric energy [36–39]. Previous studies have shown that plant MFCs can produce electricity and reduce organic pollution in wastewater simultaneously. At the same time, it is very popular to inject wastewater containing hexavalent chromium into a cathode as an electron acceptor [39–41]. However, there are few studies on the application of plant MFCs for the remediation of heavy metals in soil, such as the remediation of hexavalent chromium-contaminated soil.

With the development of MFC research, MFCs can obtain energy from wastewater so that wastewater can be utilized to obtain green and sustainable power [42–44]. In 2004, Liu et al. applied MFC technology to domestic sewage treatment and found that it could achieve the purpose of synchronous power generation, which verified that MFCs can achieve sewage purification and output energy at the same time. PMFCs are a kind of "fuel" that introduces plants into MFCs and uses their rhizosphere secretion as microorganismal anodes. In 2008, Strike et al. conducted experiments with plant microbial fuel cells, which proved the feasibility of this scheme [45], but research on PMFCs is still in its infancy. In the PMFC system, the role of plants can be divided into two categories: plants that absorb substances in the surrounding environment, such as nutrients (nitrogen and phosphorus) in sewage and toxic and harmful substances (heavy metals), which play a role in purifying the environment [46–48]; and plants that export substances to the environment through developed roots, such as organic substances (rhizosphere secretion and oxygen). In this paper, we studied the effect of plants on the treatment of chromium pollution and electricity generation in MFC systems. Plants were introduced to investigate the performance of phytoremediation of heavy metal pollution in soil by controlling the presence of plants and the type of plants.

## 2. EXPERIMENTS

All chemicals were analytical grade. The operation mode of plant microbial fuel cell reactor is circulation flow, and hydraulic retention time (HRT) is controlled by peristaltic pump. The HRT can be

divided into three conditions: 2.5h, 10h and 40H. After each condition is completed, the external circuit of the reactor shall be disconnected, and the circuit shall be reconnected after the voltage rises to the maximum and remains stable.

In the first stage of the experiment, three groups of reactors were designed: one group was planted with *Lycoris radiata*, one group was planted with *Lycoris sprengeri*, and the other group was not planted with plants and was used as a blank control group. Before planting, 500 mg potassium dichromate per kilogram soil was mixed well, and a high concentration of chromium was used to increase the treatment effect. After the first stage of the experiment, it was found that *Lycoris radiata* could adapt to an experimental environment with a high concentration of chromium and had a better power generation capacity and ability to reduce chromium pollution than *Lycoris sprengeri*. Therefore, *Lycoris radiata* was used to complete the second stage of the experiment. A mass of 20 mg and then 100 mg potassium dichromate was mixed into each kilogram of soil successively, the soil was mixed, and then *Lycoris radiata* were planted.

An equal amount of 50 mM phosphoric acid buffer salt solution, microelement solution (MgSO<sub>4</sub>: 3 g/L, CoCl<sub>2</sub>: 0.1 g/L, ZnSO<sub>4</sub>: 0.1 g/L, NaCl: 1 g/L, CaCl<sub>2</sub>: 0.1 g/L, MnSO<sub>4</sub>: 0.5 g/L, CuSO<sub>4</sub>: 0.01 g/L, KAl(SO<sub>4</sub>)<sub>2</sub>: 0.01 g/L, Na<sub>2</sub>MoV<sub>4</sub>: 0.01 g/L, H<sub>3</sub>BO<sub>3</sub>: 0.01 g/L, FeSO<sub>4</sub>: 0.1 g/L, NiCl<sub>3</sub>: 0.024 g/L, Na<sub>2</sub>WO<sub>4</sub>: 0.025 g/L) and vitamin solution are added to the reactor, which are used for the normal growth of plants and microorganisms. During the operation of the reactor, distilled water was added to the original water level every day to supplement the water that naturally evaporated. Before plants were added to the reactor, they were kept in the laboratory environment for 2 weeks for adaptation. Healthy plants of similar size were selected, cleaned with distilled water. The roots were washed carefully with deionized water taking care to protect the root hairs before planting in the reactor.

Portable hand-held dissolved oxygen meter has been used for dissolved oxygen. Total nitrogen and total phosphorus were determined with a Skalar flow analyzer.

### 3. RESULTS AND DISCUSSION

The start-up process of the reactor mainly depended on a change in voltage. In essence, the start-up process was a competition process between electricity-producing bacteria and other microbial populations in the soil [49,50]. As the electricity-producing bacteria continued to accumulate on the anode of the reactor and formed a biofilm, the voltage of the system continued to rise and stabilize. All three groups of reactors were started successfully, and all of them could generate electricity stably [51,52]. The voltage in the start-up phase is shown in Figure 1A. The start-up time of the two groups with plants was lower than that of the group without plants, which indicated that the presence of plants could accelerate the start-up of soil microbial fuel cells. However, in the white crane taro group, the highest voltage was reached faster, which may be due to the more developed root system of *Lycoris radiata*, its faster adaptation to the environment, and its large contact area with the anode.

The system voltage curve is shown in Figure 1B. In this experiment, the tested hydraulic retention times were 2.5 h, 10 hours and 40 h. Every time the HRT was changed, the reactors need to stabilize for a period of time. The voltage curve of the PMFC reactors was different from that of the ordinary MFC

because the reaction of the ordinary MFC mostly occurs in the water phase, while this experiment took place in a soil medium. When the HRT was 40 h, the maximum output voltage of *Lycoris radiata* was between 300 and 320 mV, that of *Lycoris sprengeri* was between 310 and 330 mV, and that of the non-plant group was between 250 and 270 mV. The maximum output voltage of *Lycoris radiata* was 400-410 mV, the maximum output voltage of *Lycoris sprengeri* was 370-380 mV, and the maximum output voltage of the non-plant group was 200-210 mV with increasing solution circulation speed at an HRT of 10 h.

From this figure, it could be seen that the maximum output voltage of the *Lycoris radiata* reactor was the highest and that of the reactor without plants was the lowest. This showed that although the non-plant group could also successfully initiate the microbial fuel cell and generate current, in the case of 1000  $\Omega$  external resistance, the plant groups still had the greatest advantage [53,54]. With the extension of HRT, the speed of solution circulation increased, and the voltage of each group of reactors first increased and then decreased. When the hydraulic retention time was 10 h, the maximum voltage output was obtained. The experimental results show that when the hydraulic retention time was short, the organic matter in the solution was removed from the system before being fully utilized, and the microorganisms producing electricity on the anode could not obtain sufficient nutrients. With the extension of HRT, the slow flow rate was conducive to the retention of organic nutrients in the system, and the capacity of electricity-producing bacteria improved under the supply of sufficient nutrients [55]. However, with the further extension of HRT, the maximum output voltage decreased, which was due to the slow flow of water, which led to the anode microorganisms not being supplemented in time after the "fuel" consumption was completed, the organic content in the reactor in unit time decreased, and the electricity-producing bacteria could not obtain enough "fuel" [56]. The actual measured reduced plant growth could be due to nutrient limitation for plants and/or bacteria in the reactor because of adsorption capability from activated carbon [57]. Other studies have proven that activated carbon is able to adsorb various compounds such as acetate, ammonium, phosphate, nitrate, sulphate, and metal ions [58,59].

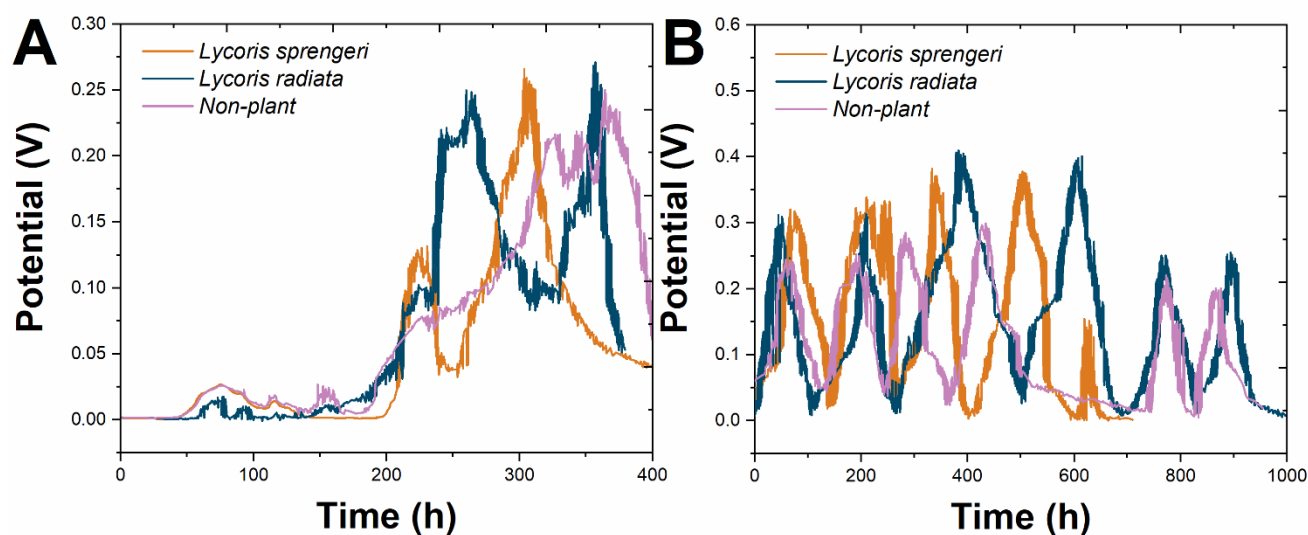


**Figure 1.** (A) Voltage diagram of start-up phase. (B) Voltage diagram during operation.

The power density of the different reactors under three kinds of HRTs was measured after the reactor reached a stable state [60]. The three groups of PMFCs were tested by the method of changing resistance. Each measurement was conducted in triplicate, and the power density curve was generated according to the results of calculation. The power density is shown in Figure 2A. It can be seen that different HRTs had a great impact on the maximum output power of the reactor. When the HRT was 40 h, the maximum output power density of *Lycoris radiata* was approximately 18.11 W/m<sup>2</sup>, the maximum output power density of *Lycoris sprengeri* was approximately 16.22 W/m<sup>2</sup>, and the maximum output power density of the non-plant group was the smallest, approximately 12.17 W/m<sup>2</sup>. The swift climb of voltage generation to the peak value is attributed to rapid microbe attraction by the anode and the fast degradation of simpler hydrocarbons in the early stages [61,62]. When the HRT was 10 h, the maximum output power density of *Lycoris radiata* was approximately 23.72 W/m<sup>2</sup>, which was 34% higher than that of the non-plant group, the maximum output power density of *Lycoris sprengeri* was approximately 20.19 W/m<sup>2</sup>, and the maximum output power density of the non-plant group was approximately 18.32 W/m<sup>2</sup>. When the HRT was 2.5 h, the output power decreased. The maximum output power density of *Lycoris radiata* was approximately 16.27 W/m<sup>2</sup>. The maximum output power density of the non-plant group was still the smallest, only 6.29 W/m<sup>2</sup>. An HRT that is too long or too short is not conducive to the further improvement of power density. Maximum output power densities were obtained for all three reactors with an HRT of 10 h.

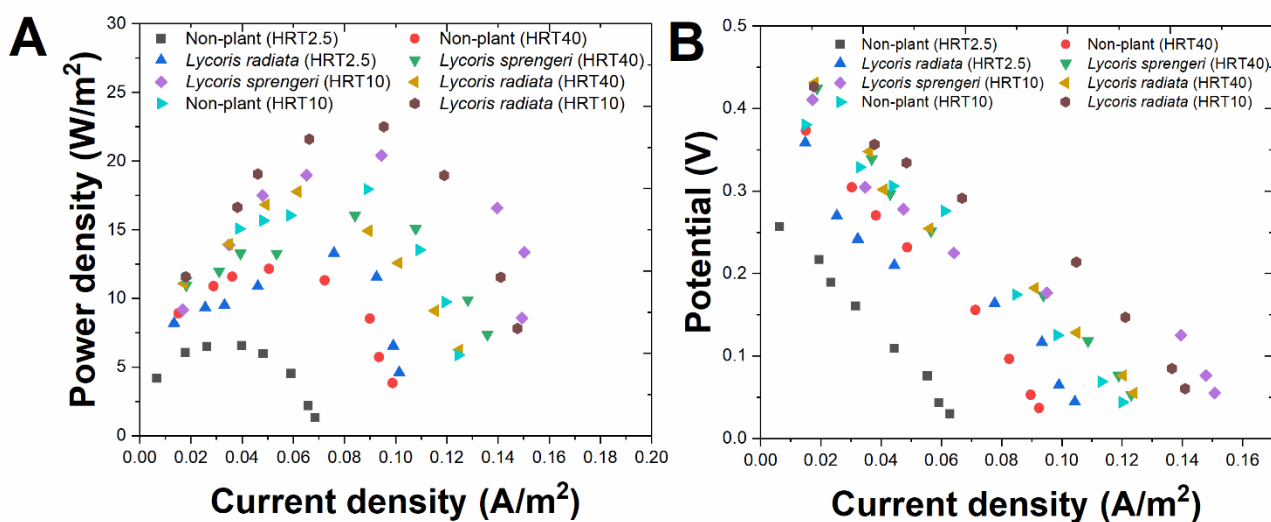


Figure 2. (A) Reactor power density curves. (B) Reactor polarization curves.

The difference in the maximum power density indicated the difference in the actual power generation performance. It could be seen that the presence of plants significantly improved the power generation performance of the reactor, especially when the hydraulic retention time was 2.5 h, and the maximum power density of *Lycoris radiata* was even 2.14 times that of the non-plant group. The possible reason is that the root exudates of the plants directly acted as electron donors for the electrode microorganisms after photosynthesis, thus increasing the energy supply. The polarization curve of the

reactor is shown in Figure 2B. It can be seen from the polarization curve that the discharge process of the three groups of reactors was relatively smooth, and there was no sharp drop in voltage when the current density reached a certain value, which indicated that the anode of the reactors has formed a stable biofilm, and the state of the three groups of reactors was relatively stable.

The oxidation number of chromium in soil is closely related to the pH value of soil. In addition, the pH value is a key factor affecting the adsorption capacity of chromium on the solid phase of soil. The influence of the pH value of a soil solution on the solubility of heavy metals further affects the enrichment of heavy metals by plants [63,64]. A high pH value is not conducive to the reduction of hexavalent chromium by soil organic matter. When the pH value is not higher than 4, 50% of hexavalent chromium will be converted into trivalent chromium and will then exist in a soil solution in the form of  $\text{Cr}(\text{OH})_3$  [65,66].

The pH change in the reactors was measured continuously from the start-up stage. Figure 3A shows that the pH of the non-plant group was always slightly higher than that of the plant groups. When the HRT was 10 h, the pH of all groups was greater than that when the HRT was 2.5 h. The pH value of the reactors was always neutral or alkaline during operation, which was different from previous research on the treatment of hexavalent chromium with MFC. Previous studies have shown that acidic conditions are favourable for chromium reduction, and a pH of 2 is the optimal condition. Only under acidic conditions can hexavalent chromium be continuously reduced to trivalent chromium. In this study, this kind of reaction could have also taken place in a neutral or alkali environment, so the reduction of chromium in our reactors mainly depended on the biocatalysis of the cathode microorganisms. In traditional methods, hexavalent chromium requires an acidic environment to dissolve in the cathode solution, and trivalent chromium is then precipitate by adjusting the pH. adjusting the pH was not needed in these reactors, which will help to reduce the cost of hexavalent chromium removal.

The content of DO in the system is related to the normal operation and treatment effect of the system. The removal of dissolved oxygen mainly includes the metabolism of microorganisms in the system, the consumption of redox reactions, and the degradation of nutrients, such as nitrogen and phosphorus and organic substances. Oxygen can be used as an electron acceptor; after the reaction,  $\text{CO}_2$  is generated and enters the atmosphere. At the same time, dissolved oxygen is closely related to the effect of changes in nitrogen and phosphorus concentrations in the reactor. Under the action of nitrifying bacteria, oxygen exists in the form of  $\text{NO}_2^-$  or  $\text{NO}_3^-$ , and when the concentration of dissolved oxygen is lower than 1.5 mg/L, nitrification will stop. In this experiment, the reactors operated via circulation flow, and the average dissolved oxygen in the influent water was 3.7 mg/L. The main sources of oxygen were from the release of plant root hairs and air reoxygenation. *Lycoris radiata* produces oxygen through photosynthesis, and part of it was released into the soil through plant transport tissue and root hair tissue. The characteristic of this kind of oxygen transfer is the formation of an aerobic area near the roots of plants, and areas further from the roots are typically anoxic and anaerobic. The large difference might be explained from two things: (1) biofilm forming at the surface, (2) difference in ion-concentration. Due to the biofilm, the top of the root system might have been sealed off from the air, preventing oxygen diffusion into the soil and thus creating an anoxic environment [67]. Figure 3B shows that the dissolved oxygen content increased with decreasing HRT. At the same time, the dissolved oxygen of *Lycoris*

*radiata* was significantly higher than that of the non-plant group. The presence of plants could improve the oxygen supply environment and increase the oxygen content in the soil.

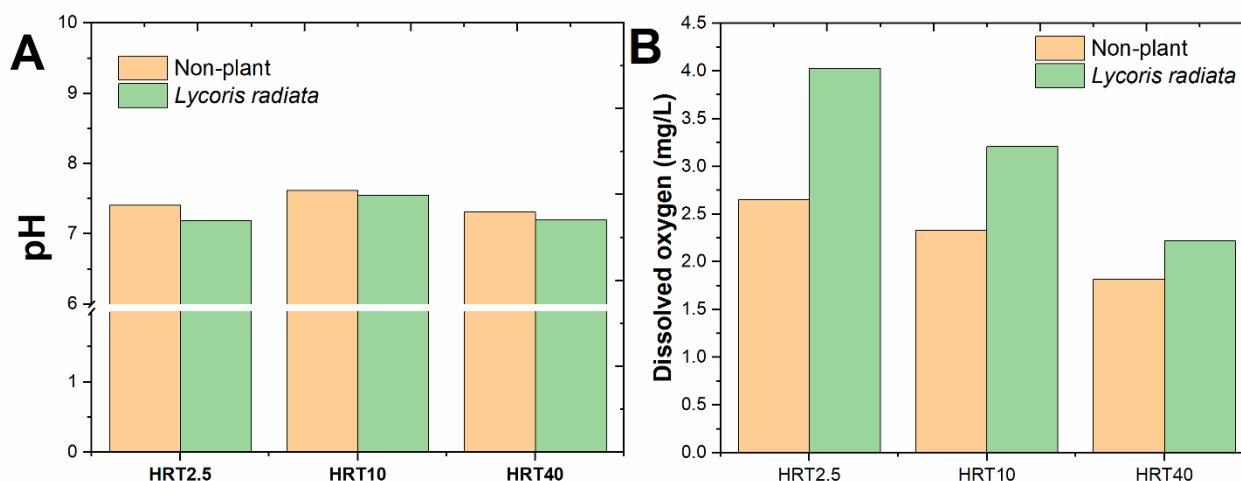


**Figure 3.** (A) pH change diagram of reactor. (B) Diagram of dissolved oxygen change of reactor.

Plant growth requires a variety of nutrients. For the growth of almost all plants, nitrogen is the primary factor limiting plant growth and yield. At the same time, nitrogen sources are essential nutrients for microbial growth. The removal rate of TN can be used as an important indicator to investigate the change in nitrogen concentration in the reactor, which can be used to characterize the denitrification efficiency and the efficiency of  $N_2$  generation. The results reported in this study indicate the feasibility of obtaining a combined process for nitrogen removal while producing electrical energy throughout a process. The continuous determination of the TN concentration in the effluent of the reactor is shown in Figure 4a. The average concentration of TN in the influent water of the reactor was 81.51 mg/L. With the continuous decrease in TN concentration during the operation of the reactor, the final effluent concentration of the plant-free group was 9.94 mg/L after 240 hours. The final concentration of the *Lycoris radiata* group was 6.22 mg/L. It can be seen that the TN of the plant group was always lower than that of the non-plant group due to the presence of plants; that is, it may be that the TN was lower due to the absorption of nitrogen by plants, transferring some of the nitrogen to the plants, and because of the enhanced stimulation of plants in microbial fuel cells, the utilization of TN in the microbial fuel cells may have increased.

Phosphorus exists in nature in a soluble or granular state. The reason for the change in total phosphorus in the reactors is that the polyphosphate bacteria gather phosphorus in an aerobic environment and release polyphosphate in the cells in an anaerobic environment. Phosphorus was eliminated from the reactors with the removal of these microorganisms that take in a large amount of phosphorus from the environment. As shown in Figure 4b, in these reactors, the TP concentration in the inlet water is 8.02 mg/L. At the initial stage, it was found that regardless of whether there was a plant TP concentration, the overall TP concentration was mainly due to the retention of soil and the electrode in the reactor. With the progress of the experiment, the concentration of total phosphorus in the group

with plants was always lower than that in the group without plants. This was not only due to the uptake of phosphorus by plants but also to the secretion of oxygen from the rhizosphere of plants, which caused aerobic, anoxic and anaerobic states to form in the soil, which was conducive to the treatment of phosphorus by phosphorus-accumulating bacteria.

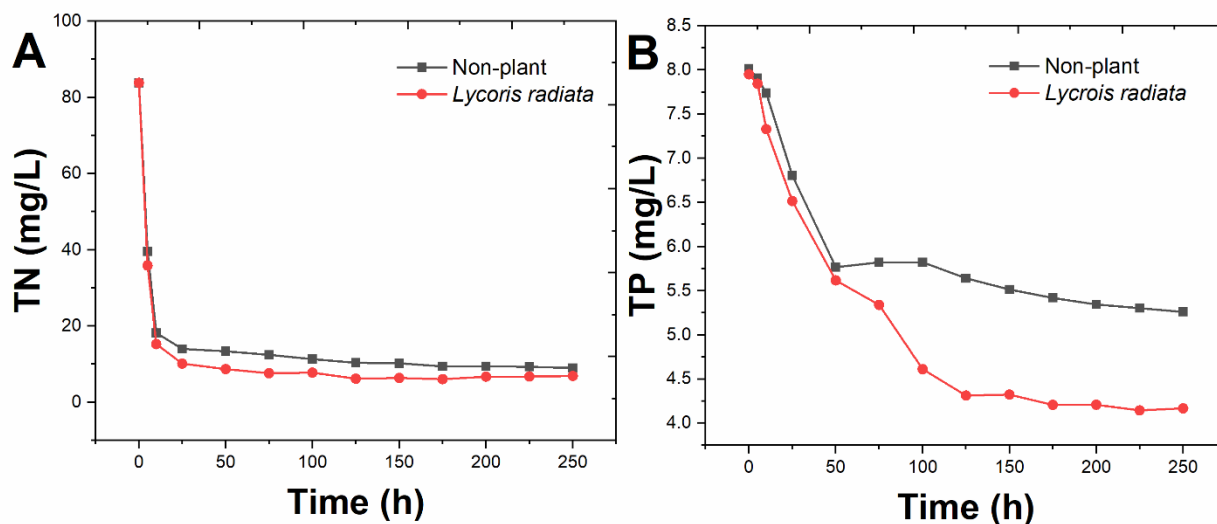


**Figure 4.** (A) Total nitrogen change diagram of the reactor. (B) Total phosphorus change diagram of the reactor.

The concentration changes in total chromium and hexavalent chromium in the reactor effluent are shown in Figure 5. In this system, hexavalent chromium was mainly removed by cathodic bioelectrochemical reduction, plant enrichment, microbial direct reduction and electrode adsorption. Common reeds had the higher translocation factor for Cr(VI) in the soil, indicating better ability to absorb Cr(VI) and then to transfer it to stems, leaves and whole plants [68]. After the operation of the reactor, it can be seen that the concentration of total chromium and hexavalent chromium decreased rapidly, which was due to the interception and adsorption of chromium by the cathode and anode materials. Later, it can be seen that the concentration of total chromium and hexavalent chromium in the effluent of the white crane taro group was significantly lower than that of the non-plant group because the root exudates of the white crane taro group provided more electronic supply for the reduction of hexavalent chromium and played a role in strengthening the bioelectrochemical transformation of hexavalent chromium to trivalent chromium. The common features of these plants are that they have a quick growth speed, high biomass, and high-density roots. Most importantly, these plants were used in phytoremediation and capable of removing pollution [69,70]. As shown in Figure 5, the adsorption of the electrode in the non-plant group reduced the chromium concentration, and at the same time, in the electrochemical system, hexavalent chromium was converted into non-toxic trivalent chromium. However, *Lycoris radiata* enhanced the reduction of hexavalent chromium due to the presence of plants, and some chromium was fixed by plant roots and enriched in plants, reducing the content of chromium in the effluent. The final concentrations of total chromium and hexavalent chromium in the *Lycoris*

*radiata* group were 0.32 mg/L and 0.16 mg/L, respectively, and those in the non-plant group were 2.86 mg/L and 2.22 mg/L, respectively.

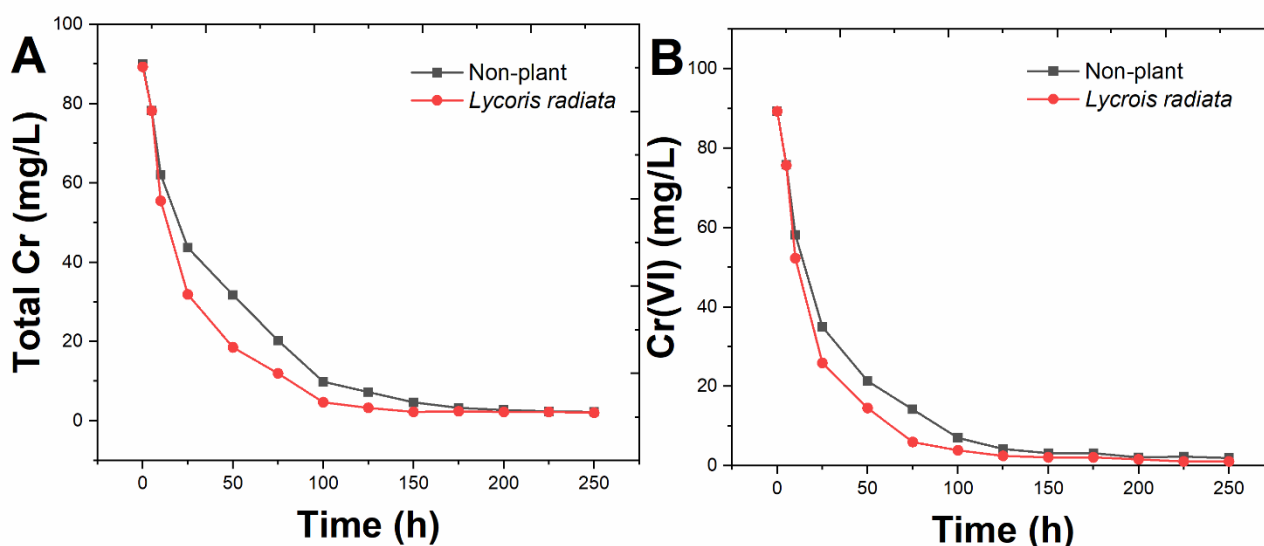


**Figure 5.** Diagram of (A) total chromium and (B) hexavalent chromium concentrations in water

#### 4. CONCLUSIONS

In this paper, two plants, *Lycoris radiata* and *Lycoris sprengeri*, were used to start PMFC reactors, and the effect of plants on the reactor was investigated at three HRTs. Operation at different HRTs showed that an effluent circulation speed that was too fast or too slow was not conducive to bioelectricity production. When the HRT was 10 hours, the power generation performance was optimal. The production of electricity by the *Lycoris radiata* group was significantly higher than that of the non-plant group. It can be seen that the presence of plants could improve the output of electric energy. The pH value of the reactor showed that the operating environment was neutral or alkaline, which was suitable for the growth of plants and soil microorganisms. The oxygen secretion in the rhizosphere created aerobic areas near the roots of plants and anaerobic and anoxic states appeared in areas farther from the roots. In addition to the absorption of nitrogen and phosphorus by plants, the TN and TP in the effluent of the cells with plants were lower than without plants.

#### ACKNOWLEDGEMENTS

This work was financially supported by the Natural Science Foundation of Jiangsu Province (Grants No. BK20151278); the Major horizontal project of Qufu normal university (Grants No. HXKJ 2019006); the Natural Sciences Foundation of Shandong Province (Grants No. ZR2016CB27); the Dachuang Project of Qufu Normal University (Grants No. 2019A022 ); the Science and Technology Project of Qufu Normal University (Grants No. xkj201608).

**References**

1. Y. Xu, W. Zhang, X. Huang, J. Shi, X. Zou, Z. Li, X. Cui, *Microchem. J.*, 149 (2019) 104022.
2. H. Xue, P. Zhou, L. Huang, X. Quan, J. Yuan, *Sens. Actuators B Chem.*, 243 (2017) 303–310.
3. W. Wang, H. Bai, H. Li, Q. Lv, Z. Wang, Q. Zhang, *J. Electroanal. Chem.*, 794 (2017) 148–155.
4. L. Zhou, D. Liu, S. Li, X. Yin, C. Zhang, X. Li, C. Zhang, W. Zhang, X. Cao, J. Wang, Z.L. Wang, *Nano Energy*, 64 (2019) 103915.
5. M. Leimbach, C. Tschaar, U. Schmidt, A. Bund, *Electrochimica Acta*, 270 (2018) 104–109.
6. L. Zhaohua, L. Cheng, X. Zhengfeng, J. Rong, X. Yu, Z. Yunnan, *Int J Electrochem Sci*, 13 (2018) 6473–6483.
7. N. Fallahpour, X. Mao, L. Rajic, S. Yuan, A.N. Alshawabkeh, *J. Environ. Chem. Eng.*, 5 (2017) 240–245.
8. S. Kuppusamy, N. Jayaraman, M. Jagannathan, M. Kadarkarai, R. Aruliah, *J. Water Process Eng.*, 20 (2017) 22–28.
9. T.K. Sari, F. Takahashi, J. Jin, R. Zein, E. Munaf, *Anal. Sci.*, 34 (2018) 155–160.
10. W. Jin, H. Du, S. Zheng, Y. Zhang, *Electrochimica Acta*, 191 (2016) 1044–1055.
11. S. Sriram, I.M. Nambi, R. Chetty, *Electrochimica Acta*, 284 (2018) 427–435.
12. W. Duan, G. Chen, C. Chen, R. Sanghvi, A. Iddya, S. Walker, H. Liu, A. Ronen, D. Jassby, *J. Membr. Sci.*, 531 (2017) 160–171.
13. Y. WANG, L. CHAI, Q. WANG, Z. YANG, R. DENG, *Trans. Nonferrous Met. Soc. China*, 27 (2017) 932–938.
14. M.A. Hussein, A.A. Ganash, S.A. Alqarni, *Polym.-Plast. Technol. Mater.*, 58 (2019) 1423–1436.
15. X. Su, A. Kushima, C. Halliday, J. Zhou, J. Li, T.A. Hatton, *Nat. Commun.*, 9 (2018) 1–9.
16. J.A. Yáñez-Varela, A. Alonzo-Garcia, I. González-Neria, V. Mendoza-Escamilla, G. Rivadeneyra-Romero, S.A. Martínez-Delgado, *Chem. Eng. J.*, 390 (2020) 124575.
17. H. Karimi-Maleh, A.F. Shojaei, K. Tabatabaeian, F. Karimi, S. Shakeri, R. Moradi, *Biosens. Bioelectron.*, 86 (2016) 879–884.
18. H. Karimi-Maleh, O.A. Arotiba, *J. Colloid Interface Sci.*, 560 (2020) 208–212.
19. S.A.R. Alavi-Tabari, M.A. Khalilzadeh, H. Karimi-Maleh, *J. Electroanal. Chem.*, 811 (2018) 84–88.
20. H. Rong, H. Hu, J. Zhang, J. Wang, M. Zhang, G. Qin, Y. Zhang, X. Zhang, *J. Mater. Sci. Technol.*, 35 (2019) 2485–2493.
21. Y. Lu, Y. Xu, H. Shi, P.Z.H. Zhang, L. Fu, *Int J Electrochem Sci*, 15 (2020) 758–764.
22. X. Yang, L. Liu, M. Zhang, W. Tan, G. Qiu, L. Zheng, *J. Hazard. Mater.*, 374 (2019) 26–34.
23. D. Lim, B. Ku, D. Seo, C. Lim, E. Oh, S.E. Shim, S.-H. Baeck, *Int. J. Refract. Met. Hard Mater.*, 89 (2020) 105213.
24. J.A. Baig, A.A. Bhutto, S. Uddin, T.G. Kazi, M.I. Khan, *J. AOAC Int.*, 101 (2018) 577–586.
25. F.P. Filice, M.S.M. Li, J.M. Wong, Z. Ding, *J. Inorg. Biochem.*, 182 (2018) 222–229.
26. M. Kodali, C. Santoro, A. Serov, S. Kabir, K. Artyushkova, I. Matanovic, P. Atanassov, *Electrochimica Acta*, 231 (2017) 115–124.
27. B. Kim, S.V. Mohan, D. Fapyane, I.S. Chang, *Trends Biotechnol.* (2020).
28. Y. Wu, X. Zhao, M. Jin, Y. Li, S. Li, F. Kong, J. Nan, A. Wang, *Bioresour. Technol.*, 253 (2018) 372–377.
29. S. Mateo, P. Cañizares, M.A. Rodrigo, F.J. Fernandez-Morales, *Chemosphere*, 207 (2018) 313–319.
30. L. Fu, Z. Liu, J. Ge, M. Guo, H. Zhang, F. Chen, W. Su, A. Yu, *J. Electroanal. Chem.*, 841 (2019) 142–147.
31. L. Fu, A. Wang, G. Lai, C.-T. Lin, J. Yu, A. Yu, Z. Liu, K. Xie, W. Su, *Microchim. Acta*, 185 (2018) 87.
32. T. Jamali, H. Karimi-Maleh, M.A. Khalilzadeh, *LWT - Food Sci. Technol.*, 57 (2014) 679–685.

33. A. Baghizadeh, H. Karimi-Maleh, Z. Khoshnama, A. Hassankhani, M. Abbasghorbani, *Food Anal. Methods*, 8 (2015) 549–557.
34. H. Karimi-Maleh, F. Karimi, M. Alizadeh, A.L. Sanati, *Chem. Rec.*, n/a (2019).
35. Y. Xu, Y. Lu, P. Zhang, Y. Wang, Y. Zheng, L. Fu, H. Zhang, C.-T. Lin, A. Yu, *Bioelectrochemistry*, 133 (2020) 107455.
36. A.T. Najafabadi, N. Ng, E. Gyenge, *Biosens. Bioelectron.*, 81 (2016) 103–110.
37. P.J. Sarma, K. Mohanty, *J. Biosci. Bioeng.*, 126 (2018) 404–410.
38. W. Yang, X. Wei, A. Fraiwan, C.G. Coogan, H. Lee, S. Choi, *Sens. Actuators B Chem.*, 226 (2016) 191–195.
39. S. Yan, J. Geng, R. Guo, Y. Du, H. Zhang, *J. Hazard. Mater.*, 333 (2017) 358–368.
40. J. Wang, X. Song, Y. Wang, B. Abayneh, Y. Li, D. Yan, J. Bai, *Bioresour. Technol.*, 221 (2016) 358–365.
41. C.-T. Wang, Y.-S. Huang, T. Sangeetha, Y.-M. Chen, W.-T. Chong, H.-C. Ong, F. Zhao, W.-M. Yan, *Bioresour. Technol.*, 255 (2018) 83–87.
42. T. Catal, H. Liu, Y. Fan, H. Bermek, *Bioresour. Technol. Rep.*, 5 (2019) 331–334.
43. S. Sarmin, B. Ethiraj, M.A. Islam, A. Ideris, C.S. Yee, Md.M.R. Khan, *Sci. Total Environ.*, 695 (2019) 133820.
44. S. Monasterio, M. Mascia, M. Di Lorenzo, *Sep. Purif. Technol.*, 183 (2017) 373–381.
45. M. Grattieri, M. Suvira, K. Hasan, S.D. Minter, *J. Power Sources*, 356 (2017) 310–318.
46. A. Vijay, M. Chhabra, T. Vincent, *Bioresour. Technol.*, 272 (2019) 217–225.
47. I. Gajda, A. Stinchcombe, J. Greenman, C. Melhuish, I. Ieropoulos, *6th Eur. Fuel Cell Technol. Appl. Piero Lunghi Conf. Exhib. EFC15 16-18 Dec. 2015 Naples Italy*, 42 (2017) 1813–1819.
48. M. Li, M. Zhou, X. Tian, C. Tan, C.T. McDaniel, D.J. Hassett, T. Gu, *Biotechnol. Adv.*, 36 (2018) 1316–1327.
49. I. Gajda, J. Greenman, I.A. Ieropoulos, *Environ. Electrochem. • Sol. Cells*, 11 (2018) 78–83.
50. Q. Tao, X. Zhang, K. Prabakaran, Y. Dai, *Bioresour. Technol.*, 278 (2019) 456–459.
51. M. Hoareau, B. Erable, A. Bergel, *Electrochem. Commun.*, 104 (2019) 106473.
52. C. Zhang, P. Liang, X. Yang, Y. Jiang, Y. Bian, C. Chen, X. Zhang, X. Huang, *Biosens. Bioelectron.*, 81 (2016) 32–38.
53. Z.-B. Wang, M. Ge, S.-C. Xiong, X.-Q. Zhu, *Ionics*, 23 (2017) 1197–1202.
54. W. Liu, L. Yin, Q. Jin, Y. Zhu, J. Zhao, L. Zheng, Z. Zhou, B. Zhu, *J. Electroanal. Chem.*, 832 (2019) 97–104.
55. U. Schröder, *ChemTexts*, 4 (2018) 19.
56. N. Shrestha, G. Chilkoor, J. Wilder, Z.J. Ren, V. Gadhamshetty, *Bioelectrochemistry*, 121 (2018) 56–64.
57. E. Menya, P. Olupot, H. Storz, M. Lubwama, Y. Kiros, *Chem. Eng. Res. Des.*, 129 (2018) 271–296.
58. L. Jourdin, S.M. Raes, C.J. Buisman, D.P. Strik, *Front. Energy Res.*, 6 (2018) 7.
59. S.E. Hale, J. Jensen, L. Jakob, P. Oleszczuk, T. Hartnik, T. Henriksen, G. Okkenhaug, V. Martinsen, G. Cornelissen, *Environ. Sci. Technol.*, 47 (2013) 8674–8683.
60. M. Kodali, R. Gokhale, C. Santoro, A. Serov, K. Artyushkova, P. Atanassov, *J. Electrochem. Soc.*, 164 (2017) H3041–H3046.
61. B. Gargouri, F. Karray, N. Mhiri, F. Aloui, S. Sayadi, *J. Chem. Technol. Biotechnol.*, 89 (2014) 978–987.
62. L. Zhao, J. Deng, H. Hou, J. Li, Y. Yang, *J. Clean. Prod.*, 221 (2019) 678–683.
63. U. Mardiana, Ch. Innocent, M. Cretin, Buchari, H. Setiyanto, R. Nurpalah, M. Kusmiati, *Russ. J. Electrochem.*, 55 (2019) 78–87.
64. J. Shen, L. Huang, P. Zhou, X. Quan, G.L. Puma, *Bioelectrochemistry*, 114 (2017) 1–7.
65. J. Chouler, I. Bentley, F. Vaz, A. O’Fee, P.J. Cameron, M. Di Lorenzo, *Electrochimica Acta*, 231 (2017) 319–326.

66. M.M. Mardanpour, M. Saadatmand, S. Yaghmaei, *Bioelectrochemistry*, 128 (2019) 39–48.
67. M. Helder, D.P.B.T.B. Strik, H.V.M. Hamelers, A.J. Kuhn, C. Blok, C.J.N. Buisman, *Bioresour. Technol.*, 101 (2010) 3541–3547.
68. A.G. Babu, J.-D. Kim, B.-T. Oh, *J. Hazard. Mater.*, 250 (2013) 477–483.
69. C.-Y. Guan, Y.-H. Tseng, D.C.W. Tsang, A. Hu, C.-P. Yu, *J. Hazard. Mater.*, 365 (2019) 137–145.
70. L. Hei, C.C. Lee, H. Wang, X.-Y. Lin, X.-H. Chen, Q.-T. Wu, *Bioresour. Technol.*, 217 (2016) 252–256.

© 2020 The Authors. Published by ESG ([www.electrochemsci.org](http://www.electrochemsci.org)). This article is an open access article distributed under the terms and conditions of the Creative Commons Attribution license (<http://creativecommons.org/licenses/by/4.0/>).